UCRL-JC-134512
PREPRINT

Subsurface Structure in Polished Fused Silica and Diamond Turned Single Crystal Silicon

Jeffrey W. Carr
Evelyn Fearon
Leslie J. Summers
Ian D. Hutcheon
Joachim K. Haack
Steve Hoskins

This paper was prepared for submittal to the
American Ceramics Society Conference
Indianapolis, IN
April 25-28, 1999

June 1999

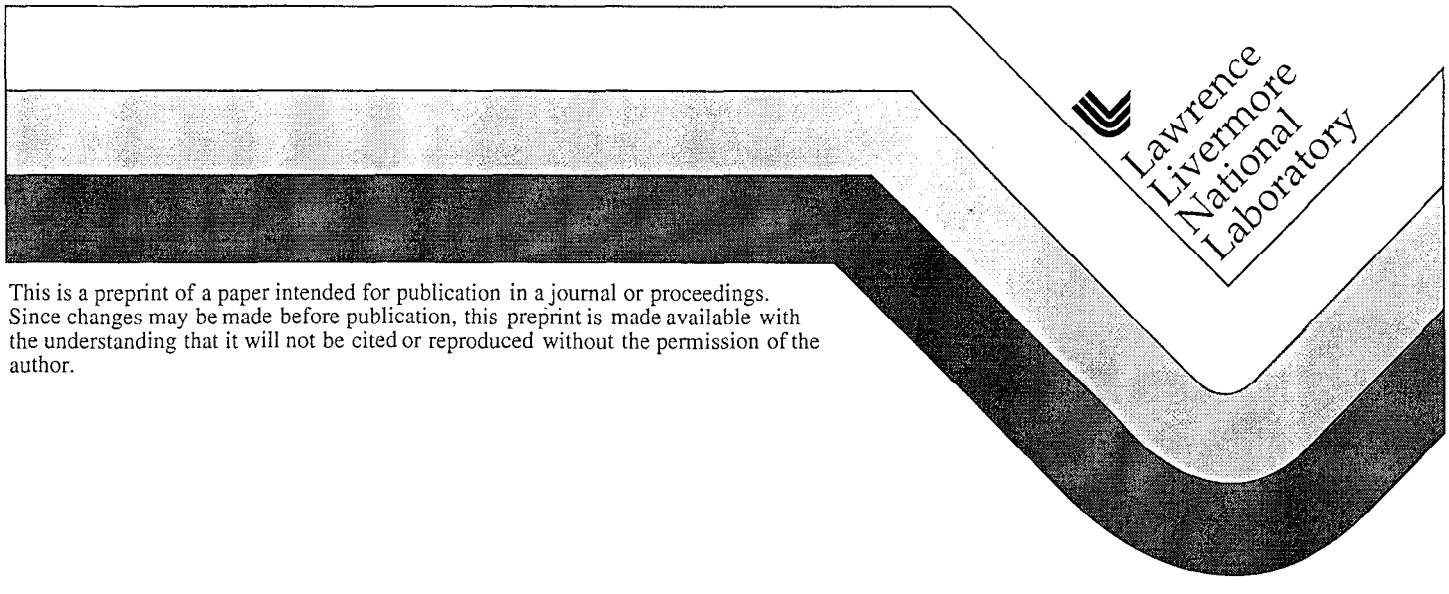

SUBSURFACE STRUCTURE IN POLISHED FUSED SILICA AND DIAMOND TURNED SINGLE CRYSTAL SILICON*

Jeffrey W. Carr, Evelyn Fearon, Leslie J. Summers,
Ian D. Hutcheon and Joachim K. Haack.
Lawrence Livermore National Laboratory
P. O. Box 808, L-537
Livermore, CA 94551

Steve Hoskins
Corning OCA
Orangewood, Ave.
Garden Grove, CA 94550

INTRODUCTION

The surface and near surface structure of glass and other optical materials is greatly influenced by the nature of the processes used to generate that surface. In high quality optics, the effects of process changes are often subtle and cannot be seen with conventional metrology. The presence of process induced damage in the near surface region is felt in a number of ways. Damage thresholds for optics subjected to high fluences are a particular problem in UV or high-powered laser systems. In high quality glass, the chemical and material composition of the outermost layer is influenced principally by the grinding, lapping and polishing processes used in fabrication. Performance in high fluence applications is often dominated by these process-induced inhomogeneties in the first few hundred nanometers of material. Each succeeding step in a process is designed to remove the damage from the previous operation. However, any force against the surface, no matter how slight will leave evidence of damage. Fabrication processes invariably create dislocations, cracks and plastic deformation between 100 nm and 500 nm below the surface. In glass polishing, the first 100 nm is comprised of material redeposited from the polishing solution. This redeposition layer is responsible for the extremely smooth

* This work was performed under the auspices of the U.S. Department of Energy by the Lawrence Livermore National Laboratory under Contract W-7405-Eng-48.

surfaces that can be generated on glass.[1] Unfortunately, this layer also conceals many flaws present in the deeper surface regions.

Single point diamond turning of many ductile materials is an accepted method for the production of mirrors. The technique has not been used extensively for the generation of transmissive components due to material limitations. One exception to this fact is the use of diamond turned single crystal silicon optics for infrared applications. As in the case of polished optics, process induced subsurface damage can cause problems in extreme applications. Since the process is dissimilar to aqueous phase glass polishing, the subsurface structure should show clear differences on comparison to fused silica. In the least, we can expect the absence of a redeposition layer. An effect of mechanical and chemical processes and the damage that is induced is to alter the chemical reactivity of the surface, enhancing corrosion and the absorptivity of the effected material. Fortunately, this enhanced reactivity can be exploited to assess the condition of the surface after lapping and polishing.

The structure of the subsurface region between 20 nm and 3 microns below the surface has been studied by atomic force microscopy (AFM). Several fused silica and silicon optical flats from various commercial manufacturers as well as the Lawrence Livermore National Laboratory optical and diamond turning shops were investigated. A number of methods can be used to etch the surface, however, the simplest is a timed immersion in a dilute HF bath. The rate of the etching process is a measure of chemical activity and infers stability of chemical bonds. Areas of stress, cracks and dislocations that occur under the redeposition layer, between 100 nm and 500 nm below the surface, will have an etch rate that differs from the bulk. Generally, the greater the stress on a bond, the faster the material will etch. However, in this experiment we have not attempted to use etch rates to assess stability; only to differentiate between different zones in the subsurface strata of an optic. The effect of force from pre-polishing grinding and lapping steps, from the polishing process itself and from diamond turning can be observed once the overlayer is removed.

In later experiments, the subsurface region was exhumed by exposing the workpiece to reactive atoms produced in a low-pressure plasma discharge. Plasma assisted chemical etching (PACE) removes the surface atoms in a damage-free process by converting them to a gas phase product that is then pumped away. If the plasma discharge is allowed to stand in one region without being tracked over the surface, material is removed in a roughly Gaussian distribution[2]. Used in this fashion, PACE can be considered a high tech ball dimple test, exposing the subsurface region for investigation. The topography of the surface can be imaged with lateral resolution below 10 nm and a vertical resolution of 0.05 nm by AFM. Subsurface structure can be quantified by a number of techniques, the simplest being the determination of average area roughness. Complimentary information can be obtained through power spectrum distributions (PSD). In the case of anisotropic

surfaces like turned silicon, it was instructive to determine roughness along a line in the direction of tool travel. Segregating X and Y roughness served to separate machine effects from the material effects of interest. To compliment the etching information on glass samples, secondary ion mass spectroscopy (SIMS) has been used to profile the distribution of elements in the subsurface region.

EXPERIMENTAL PROCEDURE

High quality fused silica optical flats, using Corning 7980 blanks, obtained from four American and European commercial sources were investigated for subsurface damage. A control group, fabricated at the Lawrence Livermore National Laboratory optical shop, was also tested. The subsurface regions were exposed by a well controlled chemical etch in a dilute HF bath. Using this approach, it is possible to remove as little as a few nanometers of material with a process control of +/- 5 %. Material was removed in increments as low as 20nm through the redeposition and damage layer, increasing to 200 nm in the bulk. To prevent excess etching times, a stronger solution was used for the removal of large amounts of material. Samples with the same etch depth from each solution were compared to ensure that each bath was performing as expected.

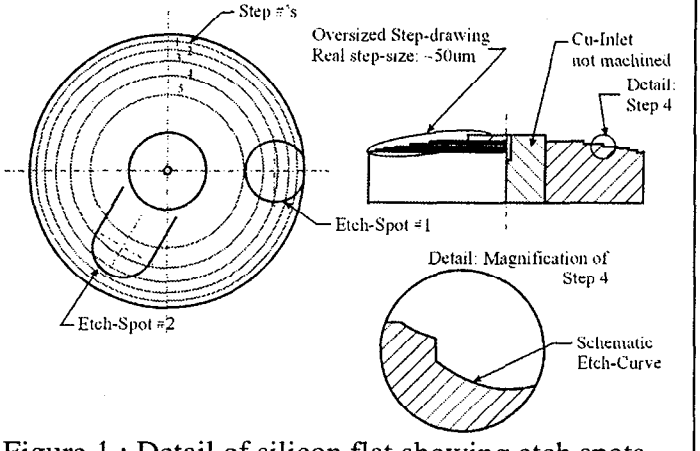

Figure 1 : Detail of silicon flat showing etch spots and zones with differing experimental conditions.

Silicon damage experiments reported in this paper were performed on a single five inch [100] single crystal silicon disk turned on the large optical diamond turning machine (LODTM) at Lawrence Livermore National Laboratory. The disk was prepared with five distinct zones cut under varying machine conditions, leaving an uncut area in the center of the sample (Fig. 1). The subsurface structure of the test piece was exposed with plasma assisted chemical etching (PACE)[2]. Etch spot #1 in Fig. 1 covered all five areas. The etch depth was determined with a 10 mm precision profilometer[3] trace along the radius of the etch spot in each zone. This trace contained a portion of both the etched and unetched region. The transition between these two areas could be clearly noted in all zones. Actual etch depth was determined by using the position of the surface in the unetched area as a reference height and determining the vertical distance between this

height and the final surface after etching. Accuracy in the measurement of the etch depths was +/- 1 nm near the beginning of the transition and up to +/- 3 nm near the end of the trace.

For the glass samples, the structure of the subsurface region between 0 nm; that shows slightly visual etching but undetectable etch depth; and 3 microns below the surface was studied by AFM. Subsurface structure was quantified using several methods of roughness analysis including fractals, power spectral density and grain size along with more traditional methods (Ra and RMS). Typically, data was collected from 30 and 5 micron square images with 60 and 10 nm resolution per pixel respectively. To avoid distortion of the data from obvious dirt in the sample window, roughness was also determined in a 10 micron area within each 30 micron image. The smaller area was chosen to be representative of the wider area while avoiding features that would skew the data. Each sample was measured a minimum of three times to lend some statistical validity to the measurements. Images of the silicon samples were collected along a radius of the etch spot in each zone. The scanned area was 10 micrometers^2 giving a lateral resolution near 20 nm. Etch depth was determined by position along the radius. An attempt was made to collect images at depths similar to the glass samples.

Secondary ion mass spectroscopy (SIMS) was used to profile the distribution of elements in the subsurface region. Elements under investigation included aluminum, barium, boron, calcium, cerium, chromium, copper, iron, magnesium, manganese, nickel, sodium and zirconium. By sputtering the surface, depth profiles were obtained for each element up to several microns into the surface.

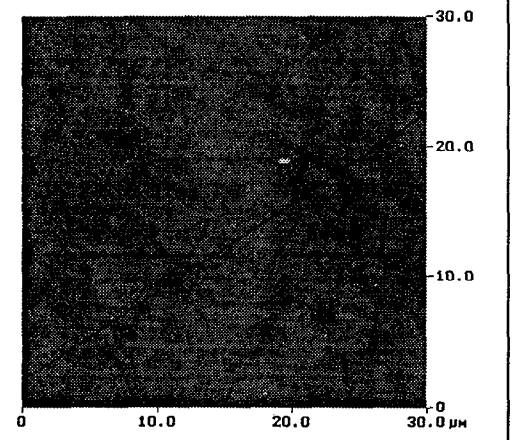

Figure 2: Glass sample; 0 nm etch depth. (undetectable etch depth).

RESULTS AND DISCUSSION

Glass Samples

AFM images of three representative depths show a qualitative difference among the surface with a slight etch (0-2 nm), a 50 nm etch depth and a 3.5 micrometer etch depth (Fig. 2-4 respectively).

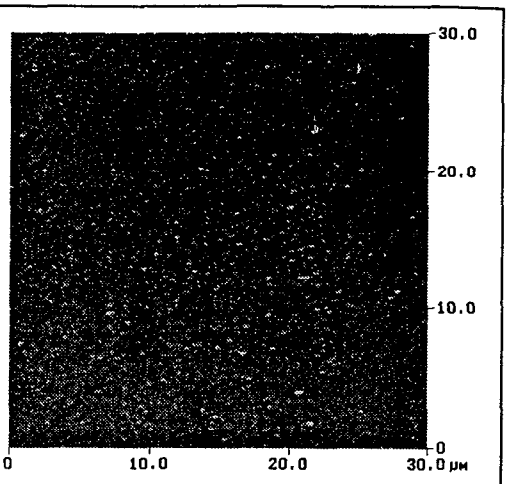

Figure 4: Glass sample; 300 nm etch detph.

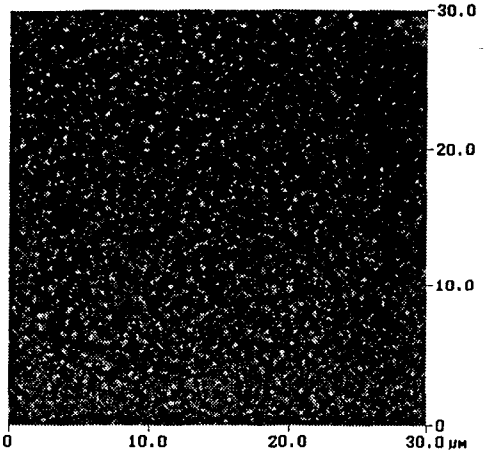

Figure 3: Glass sample; 1500 nm etch depth.

Small sleeks and scratches, evident on the surface can still be discerned at 300 nm; however, these surface features tend to disappear below 1 µm in depth. Curiously, with continued etching, new defects will appear sometimes several microns below the surface, evolve, and then shrink away (Fig. 5). Typically, these regions are in the shape of nearly round pits, less than 1 micron in diameter and 35 to 50 nm in depth. Presence of these features suggests a lower quality optic and has led to the suggestion that the glass blanks are not homogeneous in the submicron spatial region. In some of the poorer specimens, the defects link together and are

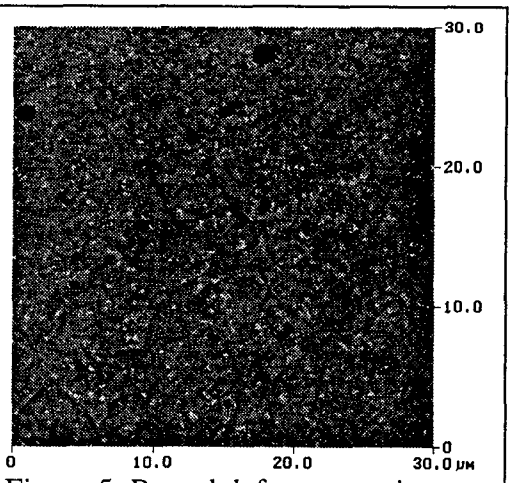

Figure 5: Round defect appearing more than 3 micron below the surface.

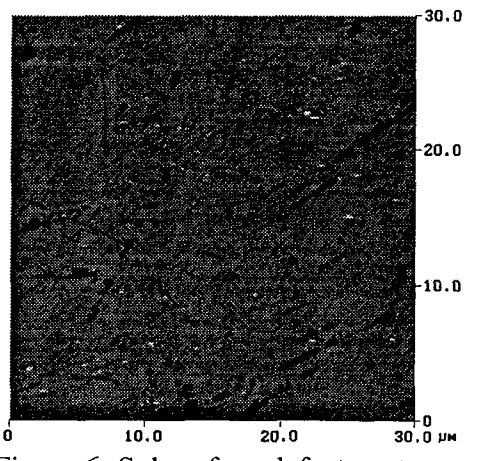

Figure 6: Subsurface defects not apparent at the surface.

imaged as long tracks (Fig. 6). Several types of structure are noted in subsurface regions and can be related to individual manufacturers (Fig. 6-8).

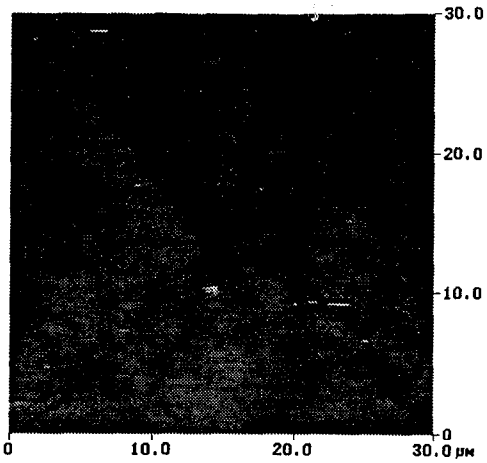

Figure 7: Subsurface defects of manufacturer A

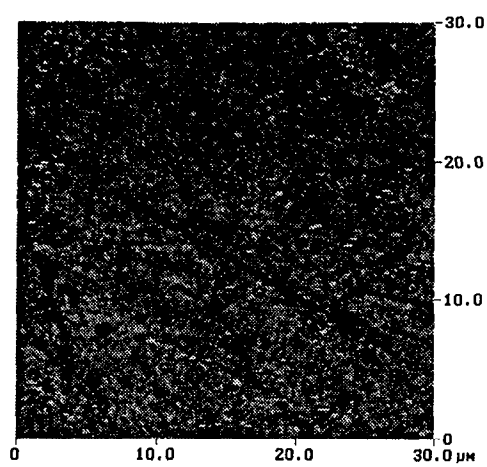

Figure 8: Subsurface defect of manufacturer B

A comparison of roughness vs etch depth for three manufacturers can be found in Table I. While the absolute values are different, each sample follows the same pattern as the etch depth is increased. A sharp increase in roughness is noted as the surface is etched from 0 to 80 nm. Past this region the surface becomes smoother until a subsurface minimum is reached around 120 nm.

Table I: Comparison of roughness for three commercial manufacturers of optical flats

Etch Depth [ηm]	Ra [ηm] A	Ra [ηm] B	Ra [ηm] C
0	0.245	0.654	1.025
40	0.422	1.245	1.772
80	0.745	2.051	2.691
120	0.489	1.875	1.803
200	0.688	1.964	2.999
300	0.902	2.516	3.756
500	1.140	3.011	4.781
1000	1.278	3.385	5.264
1500	1.484	3.696	5.840

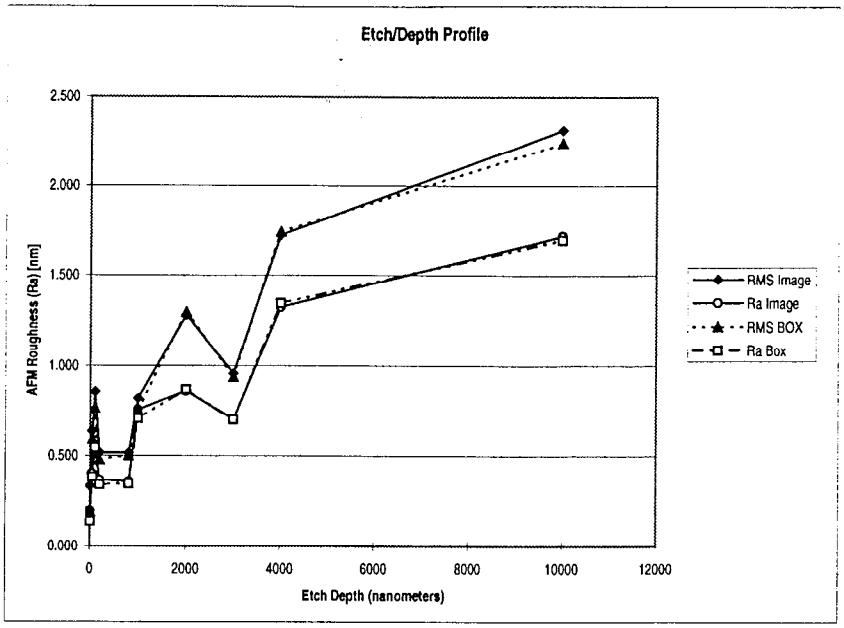

Figure 9: Typical roughness vs. depth profile for an individual optic.

Further etching causes additional roughening, increasing at a slower rate than with the first 80 nm. The Prior etching studies reported in the literature have suggested that etching should cause a surface to decrease in roughness, at least if there are any cracks[4,5]. Clearly, this is not the observation in these experiments. A typical profile for an individual optic can be seen in (Fig. 9). The initial spike in Roughness in Fig. 9 is very narrow and its position can be determined quite precisely, varying less than a few nanometers for a specific surface and less than 20 nm for all optics tested. The trend in subsurface structure for all samples can be summarized with a single plot (Fig. 10). The unexpected variation of the data in Fig. 8 between 1.0 and 4.0 micrometers can be attributed to excessive roughness readings caused by dirt on the sample surface. In

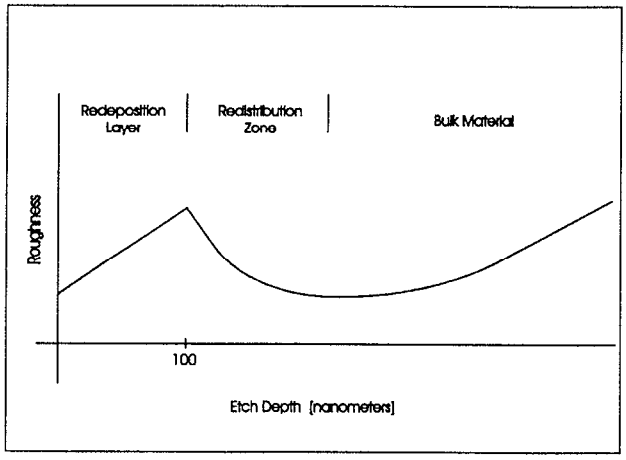

Figure 10: Summarized Schematic of Roughness vs. Depth.

corroboration with the etching data, SIMS profiling, showing the presence of water in parts per million of water vs. depth, has indicated that all of the redeposited material occurs within the first 80-100 nm of the surface. Only the bulk material is present below 100 nm (Fig. 11-12). The redeposition zone, controlled by silica chemistry, was quite constant over the range of samples studied. Correlation between the SIMS and AFM data clearly indicates that the sharp peak in the roughness data is the division between the redeposition region and a zone of plastic deformation.

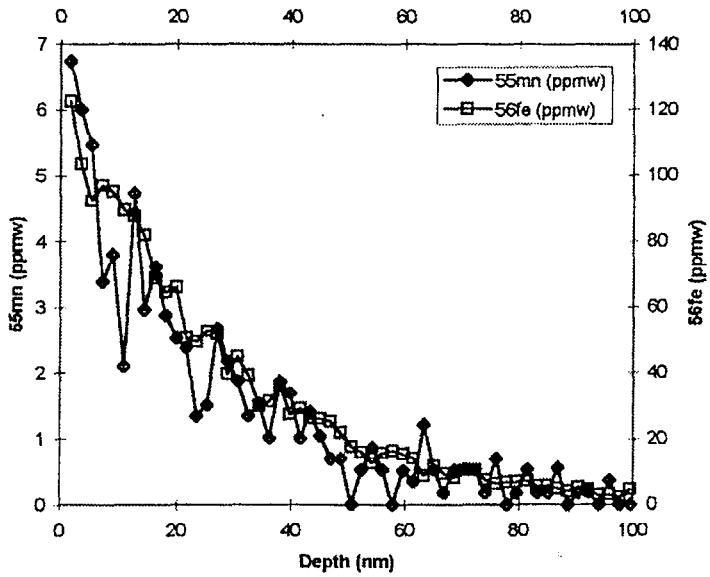

Figure 12: Presence of water in parts per million of water vs. depth for two different materials (Mn/Fe).

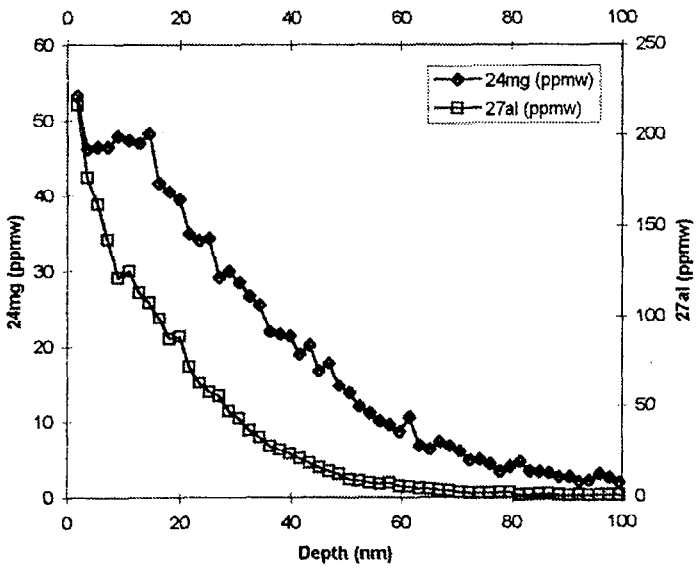

Figure 11: Presence of water in parts per million of water vs. depth for two different materials (Mg/Al).

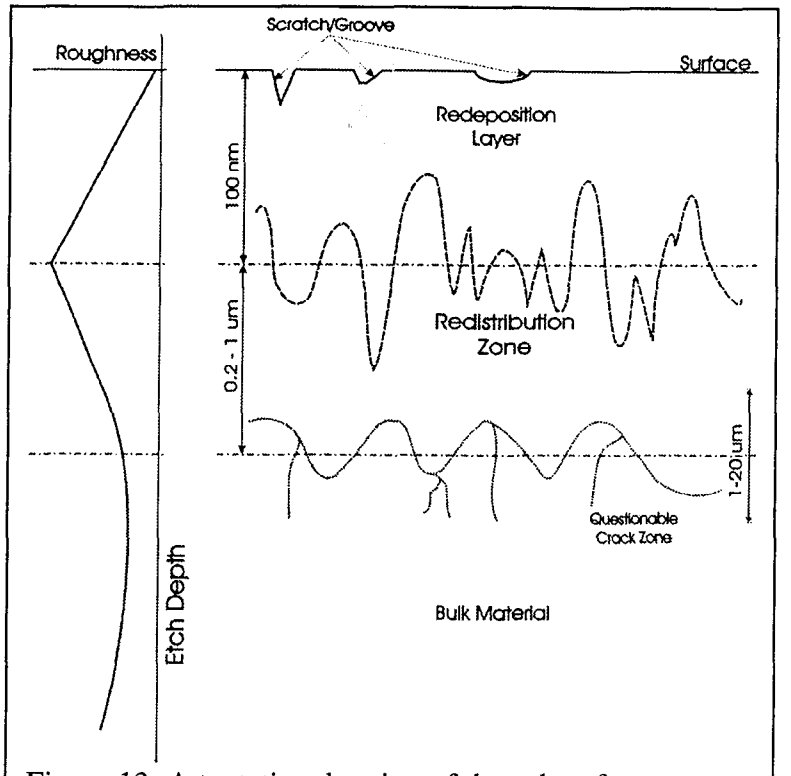

Figure 13: A tentative drawing of the subsurface structure constructed from experimental data

A tentative description of subsurface structure can be constructed from the experimental data (Fig. 13). The initial surface zone is well established as the redeposition layer. The absence of cracks immediately below this layer indicates a plastically deformed layer. The depth of the plastic or redistribution zone was found to be very process dependent, extending from 100 nm below to as much as 500 nm in some cases. This is not likely to be the limit as all samples investigated in this study were of high quality. Subsurface structure indicating the presence of cracks or voids does not appear in our samples until one or more micrometers below the surface.

Silicon Samples

AFM images of three representative depths within a single zone show a qualitative difference among a undetectable etch depth at the beginning of the etch zone, a 300 nm etch depth and a 1.5 micrometer etch depth (Fig. 14-16). Not surprisingly, the diamond turned silicon sample does not give any indication of a redeposition layer. In the initial image, the structure of the surface is directly related to operating conditions such as feed rate and tool radius. As the

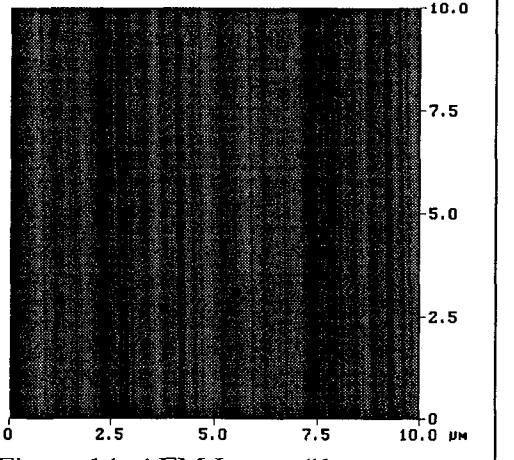

Figure 14: AFM Image #1 at undetectable etch depth

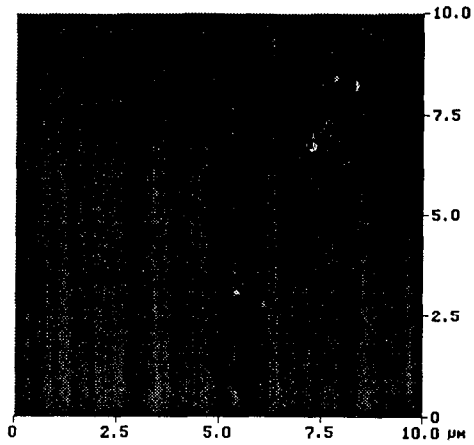

Figure 15: AFM Image #2 at etch depth of 300 nm

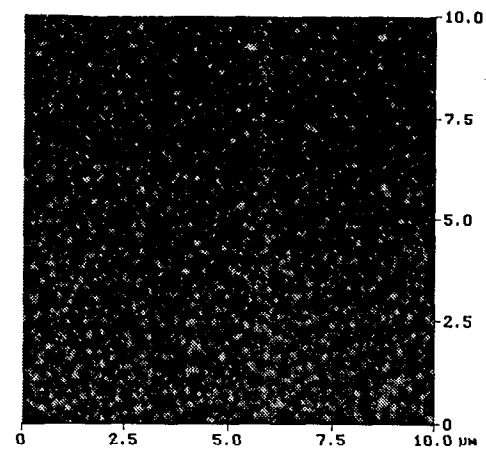

Figure 16: AFM Image #3 at etch depth of 1.5 µm

etching proceeds, the structure becomes randomized and any indication of tooling marks disappears. A plot of roughness vs. etch depth for three different zones, (see Fig. 1) fabricated by different machining conditions, shows a small peak in roughness very near to the surface of the sample (Fig. 17-19), between 15 and 30 nm below the surface. The origin of this peak is currently in question. It is unlikely to be an effect of surface roughness as all of the samples had a surface Ra between 1 and 3 nm. The thickness of the layer corresponds rather well to a typical native oxide that forms on exposed silicon so it is possible that the peak is the transition between SiO_2 and pure silicon.

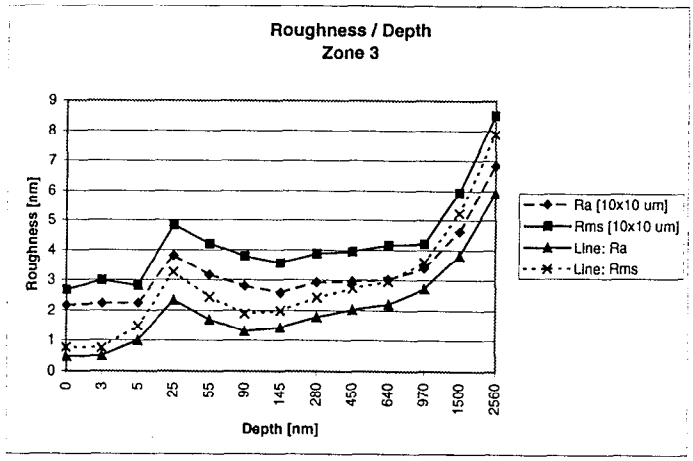

Figure 17: Roughness vs. Depth for Zone 3 for the Machined/Etched Silicon Wafer

Another possible explanation is that the peak defines the depth of the surface layer produced by turning. In order to produce a smooth or fracture free facing on silicon or other brittle work pieces, it is necessary to remove material in the ductile regime. Most materials can be removed in a ductile fashion if the depth of cut is below a certain threshold. This threshold is material and process dependant and, in the case of silicon, quite low. In order to achieve a ductile

cut within the machining parameters used to prepare our specimen, a depth of cut less than 80 nm would be required. Since it is unlikely that the true depth of cut in our experiment was that low, the surface could be expected to display some brittle behavior. Cracking was not overly evident in the AFM images. Even if the cracks were closed on the unetched surface and could not be resolved with the AFM, we would expect a shallow etch to open these cracks to the point where detection was possible. Short of causing cracks, machining could cause dislocations in the silicon. Etching would occur preferentially along the dislocations, increasing the surface roughness. The greater the number of defects, the larger the roughness increase.

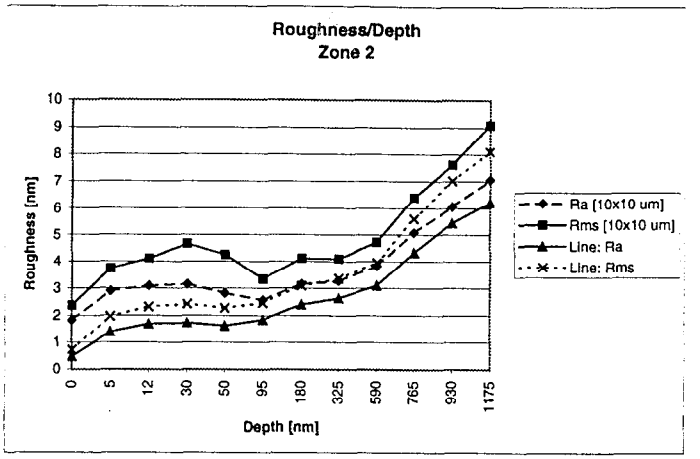

Figure 18: Roughness vs. Depth for Zone 2 for the Machined/Etched Silicon Wafer

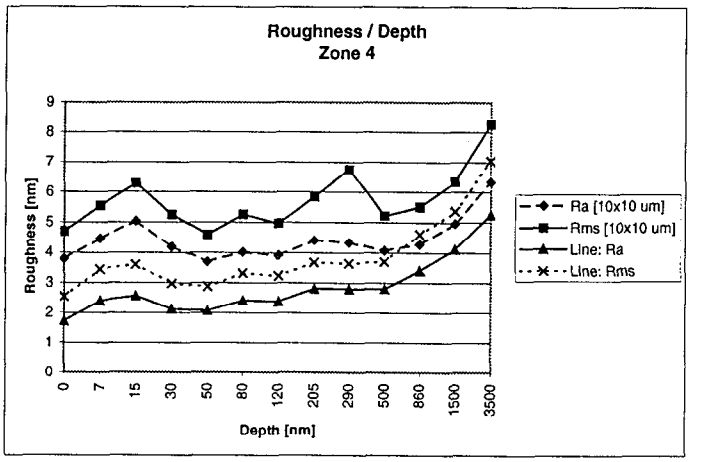

Figure 19: Roughness vs. Depth for Zone 4 for the Machined/Etched Silicon Wafer

Diamond turned parts display a directional surface structure that is dependant on the path of the tool. The roughness across the feed marks is largely due to microscopic structure in the cutting tool. However, in the direction of tool travel, details of surface structure are determined by the material properties of the work piece. Clearly, the roughness in the two orthogonal directions is different and initially we were concerned that the response to etching would also be contrary. As a result, the response of roughness to etch depth was plotted for both area and line roughness. While the response of roughness across the feed marks was not investigated, the area

and line roughness behaved in a similar fashion for all samples. Comparison of RMS and Ra roughness of area and lines in the direction of tool travel for zone 3 can be seen in Table II.

Table II: Comparison of RMS and Ra roughness for zone 3 of the SPDT sample.

Etch Depth [ηm]	Area Ra [ηm] 10x10 μm	Area RMS [ηm] 10x10 μm	Line Ra [ηm]	Line RMS [ηm]
0	2.164	2.675	0.4813	0.7681
3	2.236	2.988	0.5076	0.7625
5	2.243	2.813	1.0036	1.4842
25	3.823	4.852	2.3356	3.2569
55	3.174	4.214	1.6954	2.4447
90	2.800	3.796	1.3077	1.8864
145	2.585	3.567	1.4323	1.9892
280	2.927	3.890	1.7834	2.4275
450	2.956	3.962	2.0318	2.7281
640	3.017	4.177	2.2134	2.9602
970	3.397	4.218	2.7245	3.5961
1500	4.635	5.955	3.8235	5.2429

CONCLUSIONS

The assessment of subsurface structure by AFM is a promising technique for the determination of process induced distortion. To a certain degree, the history of the process is written in the part. Certain features in the optic can be consistently related to specific manufacturers. While mainly focusing on optics, either polished or single point diamond turned, the technique can be used to evaluate process-induced damage for many precision components where surface integrity is of interest.

REFERENCES

1.L. M. Cook, Chemical Processes in Glass Polishing, J. Non-Cryst. Sol.120 (1990) 152.

2.a)L. D. Bollinger and C. B. Zarowin, Part 1, Proc. SPIE, **966**, 82 (1988); b) L. D. Bollinger and C. B. Zarowin, Part 2, Proc. SPIE, **966**, 91 (1988); c) S. J. Hoskins and B. Scott, Proc. SPIE, **2542**, 220 (1995); d) S. J. Hoskins and B. Scott, Proc. SPIE, **2542**, 235 (1995)

3.Digital Instruments series 5000 AFM with a Nanomotion profiling stage

4.G.A.C.M. Spierings, J. Mater. Sci., 28 (1993) 6261; b) G.A.C.M. Spierings, J. Van Dijk, J. Mater. Sci., 22 (1987) 1869.

5.P.N. Homer, B.J. Crawford, Glass Technol. 11 (1970) 10.